Macromolecules **1993,** *26,* 1265–1269

Kinetic Analysis of Triplet Energy Migration in Poly[(2-naphthylalkyl methacrylate)-*co*-(methyl methacrylate)]s and Poly[(9-phenanthrylmethyl methacrylate)-*co*-(methyl methacrylate)] Solid Films

Hideaki Katayama, Tsutomu Tawa, Gregory W. Haggquist, Shinzaburo Ito, and Masahide Yamamoto*

Department of Polymer Chemistry, Faculty of Engineering, Kyoto University, Sakyo-ku, Kyoto 606, Japan

Received September 14, 1992

ABSTRACT: Triplet energy migration in chromophoric polymer films has been investigated by phosphorescence spectroscopy. Poly[(2-naphthylalkyl methacrylate)-*co*-(methyl methacrylate)] and poly[(9-phenanthrylmethyl methacrylate)-*co*-(methyl methacrylate)] films show phosphorescence spectra from "triplet trap sites". The emission is slightly red-shifted from the monomer phosphorescence with a vibrational structure which is different from that of the triplet excimer. The energy migration rate in these systems is complex since the trap sites have various energy levels depending on the amplitude of interaction energies. The kinetic analysis was made on the basis of Bässler's model in which the site energies have a Gaussian distribution. The simulations are in good agreement with experimental data in a temperature range of 115–165 K. The results provide strong evidence for the hopping mechanism of trapped excitons among a distribution of energy sites for a particular energy level.

Introduction

Energy transfer and energy migration are important primary processes of photochemical reactions.[1,2] There are two types of energy transfer: Förster type (singlet) and Dexter type (triplet).[3,4] The Dexter type energy transfer is often utilized in photosensitive polymers because of the long lifetime of the triplet state. However, the behavior of triplet energy transfer in polymers has not been fully understood, because of experimental difficulties such as weak emission due to efficient nonradiative deactivation. The triplet energy migration occurs by a short-range interaction involving the overlap of the electron clouds from each chromophore.[3] This means that the effective energy transport is able to take place only in concentrated chromophoric systems. In such systems, excited chromophores are often involved in interchromophore interactions and form stabilized sites such as an excimer site or a trap site.[5–11]

In previous papers we reported two types of triplet-state behavior for several kinds of chromophoric polymer films.[12–15] The copolymer films containing carbazole chromophores and benzene chromophores show broad and widely red-shifted phosphorescence spectra. This emissive species was assigned to a triplet excimer.[12,13] The triplet excimer acts as a deep trap site for the energy migration; hence, the triplet exciton once captured by the excimer site cannot be released to the mobile state. On the other hand, the copolymer films containing phenanthrene or naphthalene chromophores show slightly red-shifted phosphorescence spectra with vibrational band structure, and the shape was different from the excimer emission.[11,14,15] This different type of band was termed a "triplet trap site" to distinguish it from the triplet excimer. The energy migration rate in the phenanthrene-containing polymer film (trap-forming type) is slower than that in the carbazole-containing polymer film (excimer-forming type). The triplet trap sites of phenanthrene and naphthalene chromophores act as shallow traps for energy migration. The trapped exciton can be thermally released from the trap site, and triplet energy migration occurs with iterative trapping and detrapping processes. So, the detrapping process is the rate-determining process. Multiple rate constants for triplet energy migration were observed by the phosphorescence decay measurement. This indicated that the energy levels of the trap sites have a distribution of energies in the solid films.

Many workers have suggested mechanisms to describe the complicated relaxation processes of excited states.[16–28] Bässler et al. analyzed the migration process of triplet excitons in organic layers by Monte Carlo simulation.[29] They assumed exciton hopping among a distribution of energy sites which is a Gaussian function. They also reported that this distribution of site energies (DOS) model is adequate for expressing the charge transport, photophysical hole burning, singlet energy migration, and thermally induced transform of spiropyran in polymer solids.[30] In this study, the DOS model was applied to our polymer systems and the adequacy of the model was examined by the phosphorescence decay analysis.

Experimental Section

Materials. Synthetic methods for poly[(2-naphthylmethyl methacrylate)-*co*-(methyl methacrylate)] (P(NMMA-*co*-MMA)), poly[(2-naphthylethyl methacrylate)-*co*-(methyl methacrylate)] (P(NEMA-*co*-MMA)), poly[(2-naphthylpropyl methacrylate)-*co*-(methyl methacrylate)] (P(NPMA-*co*-MMA)), and poly[(9-phenanthrylmethyl methacrylate)-*co*-(methyl methacrylate)] (P(PhMMA-*co*-MMA)) were described previously.[13,15] 1,4-Dibromonaphthalene (DBN; Kantou Chemical Industry Co., Ltd.) was recrystallized from methanol and was used as a triplet energy acceptor. 3,6-Dibromo-9-ethylcarbazole (DBCz), a triplet sensitizer, was synthesized from 9-ethylcarbazole according to the procedure in the literature.[31]

The properties of these materials are listed in Table I.

Sample Preparation. The copolymers were dissolved in dichloromethane or benzene (spectrophotometric grade; Dojindo Laboratories) in a quartz cell, and the solutions were deaerated by several freeze–thaw cycles to a final pressure of less than 5×10^{-6} Torr. Copolymer films were cast in a quartz cell by gradual evaporation of solvent under reduced pressure. The cell was sealed after keeping the film in vacuo. DBN-doped films were prepared in the same manner by addition of DBN to the casting solution. The concentration of DBN was adjusted to be 8×10^{-3} mol/L. As for poly[(2-naphthylalkyl methacrylate)-*co*-(methyl methacrylate)]s (P(NAMA-*co*-MMA)s), DBCz was used as a

0024-9297/93/2226-1265$04.00/0

Table I
Composition of Polymers, Average Distance between Chromophores (D), Singlet Energy Level (E_S), and Triplet Energy Level (E_T)

	Np content (mol %)	Ph content (mol %)	D^a (nm)	E_S^b (kJ/mol)	E_T^b (kJ/mol)
P(NMMA-*co*-MMA)	21.3		0.940	386	254
P(NEMA-*co*-MMA)	19.2		0.974	386	254
P(NPMA-*co*-MMA)	19.6		0.975	386	254
P(PhMMA-*co*-MMA)		18.6	1.00	346	260
DBN				374	237
DBCz				333	280

[a] Calculated by $D = n^{-(1/3)}$, where n is the average number of chromophores per unit volume. [b] Calculated from the 0–0 transition band.

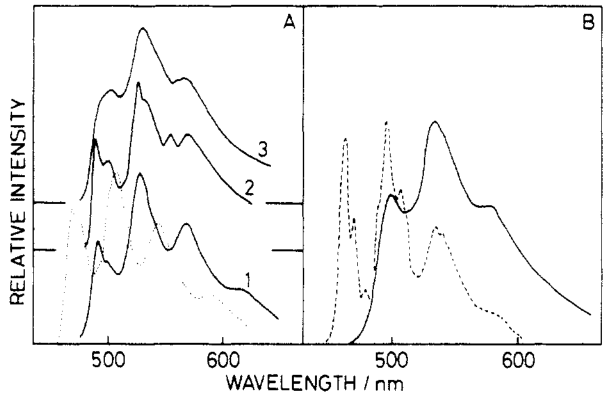

Figure 1. (A) Phosphorescence spectra of P(NAMA-*co*-MMA) films at 77 K: (1) P(NMMA-*co*-MMA), (2) P(NEMA-*co*-MMA), and (3) P(NPMA-*co*-MMA). The dotted line represents the phosphorescence spectrum of 2-methylnaphthalene in MTHF at 77 K. The samples are excited at 277 nm. (B) Phosphorescence spectrum of a P(PhMMA-*co*-MMA) film at 77 K. The broken line represents the phosphorescence spectrum of phenanthrene in MTHF at 77 K. The samples are excited at 330 nm.

triplet sensitizer to avoid direct excitation of DBN. This was done because the absorption band of the naphthalene chromophore overlaps that of DBN. The singlet level of DBCz is lower than that of naphthalene, but the triplet level of DBCz is much higher than that of naphthalene. So the DBCz can be selectively excited in a wavelength range of 330–350 nm, and the produced triplet energy of DBCz transfers immediately to the surrounding naphthalene moieties of the copolymers. DBCz-doped films were prepared in the same manner as DBN-doped films by addition of DBCz to the casting solution. The concentration of DBCz was 10^{-2} mol/L.

Measurements. Steady-state phosphorescence spectra were obtained with a Model 850 Hitachi spectrofluorophotometer fitted with a phosphorescence attachment. Phosphorescence decay curves were measured with a phosphorimeter assembled in our laboratory. A nitrogen laser (NDC Co., JH-500) was used as an excitation light source, and phosphorescence decay was detected by a gated-photomultiplier (Hamamatsu, R1333). Details of the systems were described elsewhere.[12] The temperature was regulated by a cryostat.

Results and Discussion

Spectroscopic Measurements. Figure 1 shows the phosphorescence spectra of P(NAMA-*co*-MMA) films (Figure 1A) and a P(PhMMA-*co*-MMA) film (Figure 1B). The copolymer spectra are slightly red-shifted with vibrational bands compared to isolated chromophores.

Figure 2 shows the temperature dependence of phosphorescence spectra of a P(NEMA-*co*-MMA) film containing DBCz and DBN. The excitation wavelength is 330 nm; i.e., DBCz is selectively excited. Observed phosphorescence spectra show only the DBN phosphorescence over the measured temperature range. This result indicates that the triplet energy of DBCz transfers completely to naphthalene moieties of the copolymer, then migrates among naphthalene chromophores, and finally transfers to DBN with a high efficiency. The kinetic equations for these processes are described as follows:

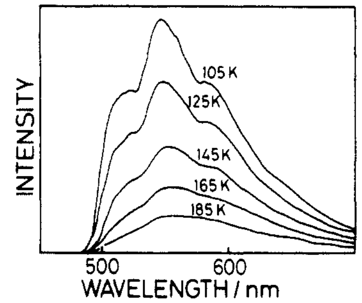

Figure 2. Temperature dependence of phosphorescence spectra of DBN-doped P(PhMMA-*co*-MMA). The sample is excited at 330 nm.

$$T_{DBCz} \xrightarrow{k_{ST1}} S_{0\,DBCz} + h\nu/\text{heat} \tag{1}$$

$$T_{DBCz} \xrightarrow{k_{tr1}} T_{Np} \tag{2}$$

$$T_{Np} \xrightarrow{k_{ST2}} S_{0\,Np} + h\nu/\text{heat} \tag{3}$$

$$T_{Np} \xrightarrow{k_{tr2}} T_{DBN} \tag{4}$$

$$T_{DBN} \xrightarrow{k_{ST3}} S_{0\,DBN} + h\nu/\text{heat} \tag{5}$$

where T and S_0 represent the excited triplet state and the ground state, respectively, and the suffix is the name of the compound, k_{tr} is the rate of energy transfer, and k_{ST} is the intrinsic rate of deactivation to the ground state. The k_{tr2} includes energy migration among naphthalene chromophores and energy transfer to DBN. In this system, $k_{tr1} \gg k_{ST1}$ and $k_{tr2} \gg k_{ST2}$, so only the DBN phosphorescence was detected.

Figure 3 shows the rise and decay profiles of the acceptor phosphorescence in a P(NMMA-*co*-MMA) film at various temperatures. The rise time becomes faster with increasing temperature. This behavior indicates that the rate of the detrapping process is thermally accelerated. Other polymer films also show a trend in the rise and decay curves analogous to that of P(NMMA-*co*-MMA).

Simulation by the Bässler Model. Bässler et al. analyzed the triplet energy migration in amorphous organic layers. They assumed that the energy migration in those systems occurs through exciton hopping among the sites which exhibits a Gaussian distribution of site energies. They obtained the exciton hopping frequency, $\nu(t)$, at time t, by a Monte Carlo simulation as follows:

$$\nu(t) = \nu_0(t/t_0)^{\alpha-1} \tag{6}$$

where α is the dispersion parameter and t_0 is a characteristic time. In their simulation, 40 × 40 × 40 of sites were considered. Each site has a different energy level which is distributed in a Gaussian function. The distance between sites is taken to be 1.0 nm. In our systems the average interchromophore distances are 0.9–1.0 nm, which corresponds well with Bässler's model. Bässler et al.

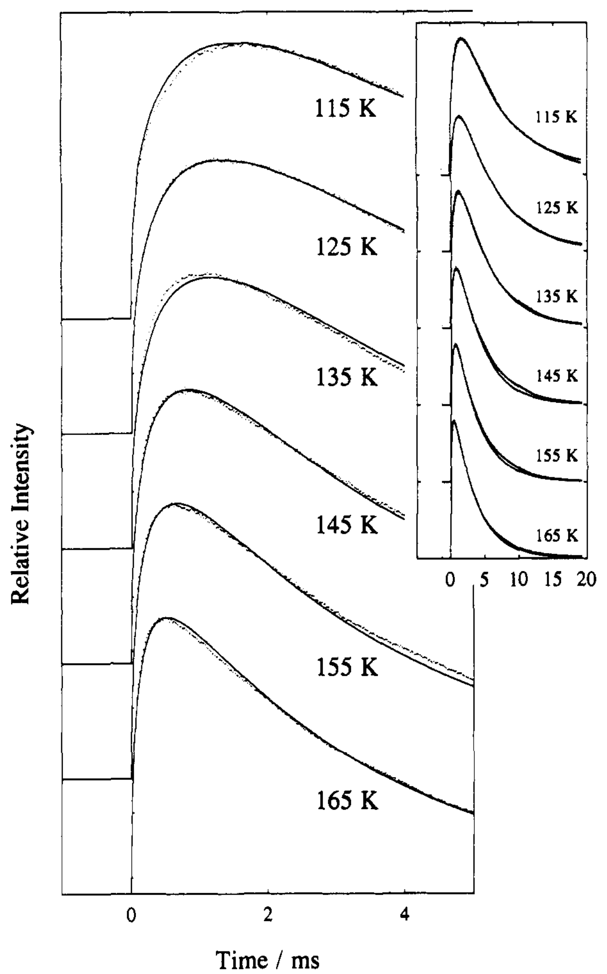

Figure 3. Temperature dependence of the rise and decay curves of DBN phosphorescence in P(NMMA-*co*-MMA). The emission was detected at 545 nm. The solid lines represent the results of calculation based on the DOS model with ν_0 = 22.74 μs^{-1} and α = 0.421 (115 K), 0.468 (125 K), 0.497 (135 K), 0.554 (145 K), 0.589 (155 K), and 0.628 (165 K).

represented α empirically as

$$\alpha^{-1} = (\sigma/4kT)^2 + 1 \tag{7}$$

where σ is the width of the Gaussian distribution.

We used DBN as an energy acceptor. The triplet energy level of the acceptor is low enough compared with that of the chromophores being excited; hence, DBN acts as a deep trap from which the triplet exciton cannot be released. The equation for the excited triplet naphthalene or phenanthrene chromophore is given by

$$\frac{\mathrm{d}D(t)}{\mathrm{d}t} = -c\nu(t)\,D(t) - \frac{D(t)}{\tau_D} \tag{8}$$

where $D(t)$ is the number of excited chromophores, τ_D is the intrinsic lifetime of the chromophore, and c is the acceptor concentration. Similarly, the number of excited acceptors, $A(t)$, is written as follows:

$$\frac{\mathrm{d}A(t)}{\mathrm{d}t} = c\nu(t)\,D(t) - \frac{A(t)}{\tau_A} \tag{9}$$

where τ_A is the lifetime of the acceptor. If $\tau_D^{-1} \ll \nu(t)$, eq 8 can be simplified as

$$\frac{\mathrm{d}D(t)}{\mathrm{d}t} = -c\nu(t)\,D(t) \tag{10}$$

As mentioned above, our systems satisfy the conditions $k_{ST2} \ll k_{tr2}$, so $\tau_D^{-1} \ll \nu(t)$. Then we obtained $A(t)$ from eq 9, eq 10, and eq 6 as follows.

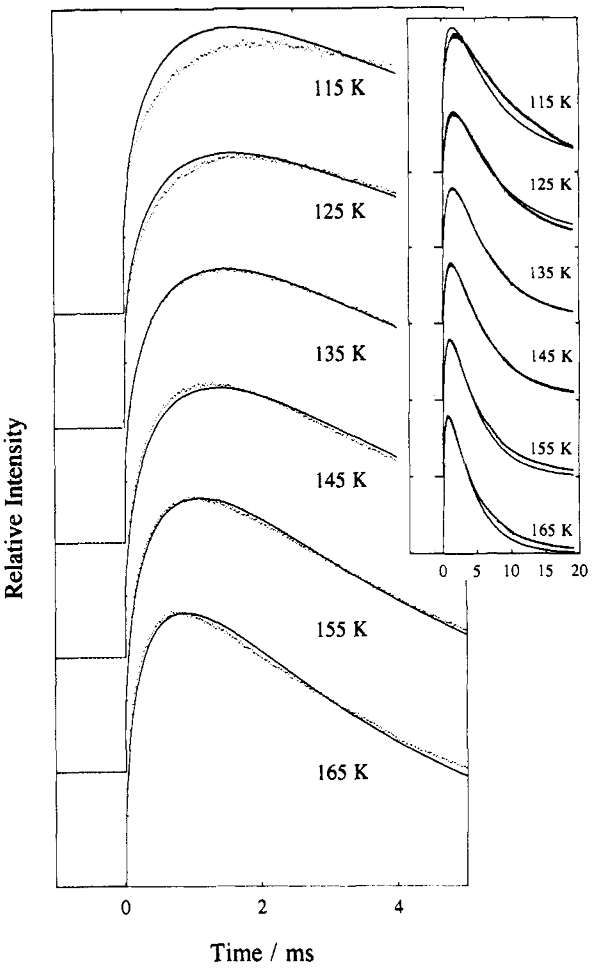

Figure 4. Temperature dependence of the rise and decay curves of DBN phosphorescence in P(NEMA-*co*-MMA). The emission was detected at 545 nm. The solid lines represent the results of calculation based on the DOS model with ν_0 = 19.42 μs^{-1} and α = 0.353 (115 K), 0.408 (125 K), 0.453 (135 K), 0.477 (145 K), 0.502 (155 K), and 0.532 (165 K).

$$A(t) = cD_0 \exp\left(-\frac{t}{\tau_A}\right)\int_0^t \left[\nu_0\left(\frac{T}{t_0}\right)^{\alpha-1} \exp\left\{\frac{-c\nu_0 t_0}{\alpha}\left(\frac{T}{t_0}\right)^{\alpha} + \left(\frac{T}{\tau_A}\right)\right\}\right] \mathrm{d}T \tag{11}$$

Curve fitting was performed with the parameters ν_0 and α by use of eq 11, where τ_A was determined by the measurement of the phosphorescence lifetime of DBN doped in a PMMA film at various temperatures. The constant t_0 was fixed to 10 ns according to the procedure of Bässler et al. Figures 3–6 show the results of the curve fitting. The calculated curves fit fairly good over the range of temperature from 115 to 165 K for P(NMMA-*co*-MMA) (Figure 3) and P(PhMMA-*co*-MMA) (Figure 6) and from 125 to 165 K for P(NEMA-*co*-MMA) (Figure 4) and P(NPMA-*co*-MMA) (Figure 5) but deviate at temperatures lower than 115 K and higher than 165 K. We employed a single dispersion parameter α for describing the decay profile for the entire time range, and this could be the reason for the deviation at low temperatures. Better fits can be obtained if we use a time-dependent α, for instance, one value for the short time region and one value for the long time region. This means that the distribution of energies for the triplet level becomes wider. On the other hand, the deviation at higher temperatures is probably due to the peculiar situation of our system. In our system we used an emissive energy acceptor DBN for probing

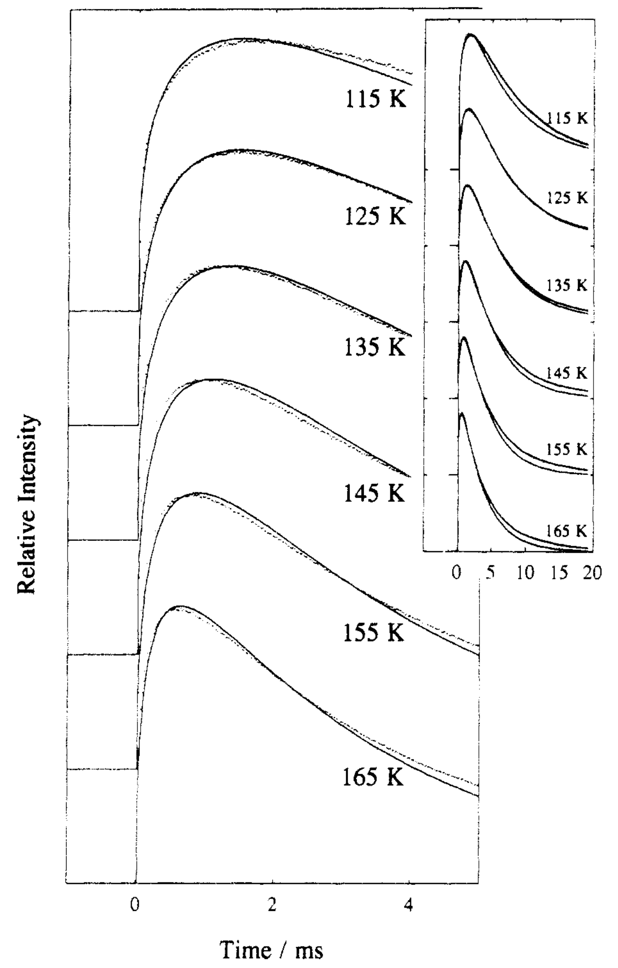

Figure 5. Temperature dependence of the rise and decay curves of DBN phosphorescence in P(NPMA-*co*-MMA). The emission was detected at 545 nm. The solid lines represent the results of calculation based on the DOS model with $\nu_0 = 23.30\ \mu s^{-1}$ and $\alpha = 0.370$ (115 K), 0.399 (125 K), 0.454 (135 K), 0.501 (145 K), 0.542 (155 K), and 0.589 (165 K).

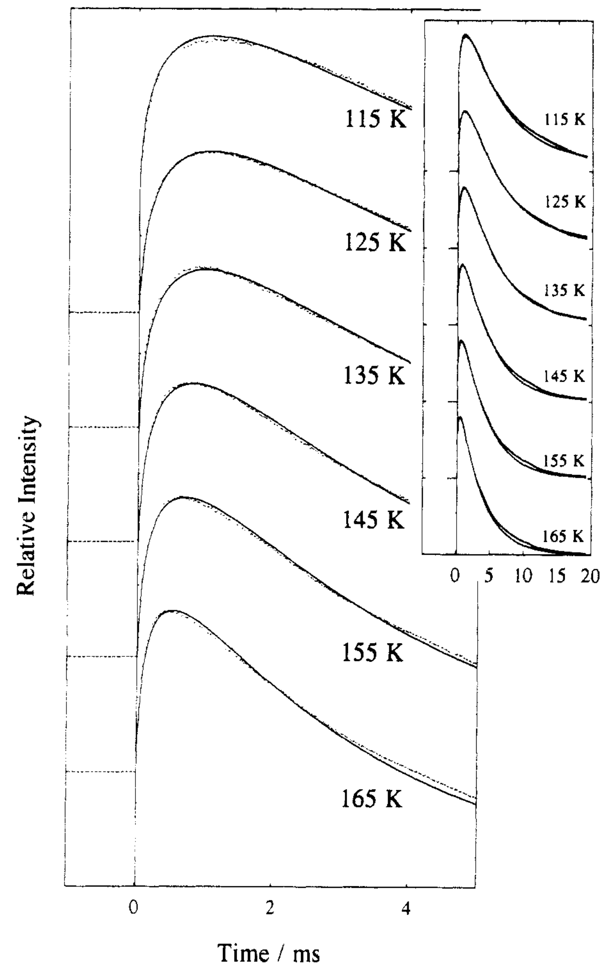

Figure 6. Temperature dependence of the rise and decay curves of DBN phosphorescence in P(PhMMA-*co*-MMA). The emission was detected at 545 nm. The solid lines represent the results of calculation based on the DOS model with $\nu_0 = 59.10\ \mu s^{-1}$ and $\alpha = 0.299$ (115 K), 0.331 (125 K), 0.375 (135 K), 0.424 (145 K), 0.451 (155 K), and 0.492 (165 K).

energy migration processes. The triplet energy of DBN is lower than those of naphthalene and phenanthrene chromophores, but, at high temperatures, thermal energy is large enough to give rise to back energy transfer from DBN to the donor chromophores. Indeed, we have already reported thermal detrapping from DBN in P(PhMMA-*co*-MMA) films at temperatures higher than 170 K.[14] Hence, the prerequisite for eq 11 would fail under such circumstances.

A plot of α vs T for each sample is displayed in Figure 7. The values of α increase with increasing temperature as expected from eq 7. The lines in Figure 7 were fitted to, using eq 7, σ as an adjustable parameter. The values obtained for σ are listed in Table II. The stabilization energies, $\Delta\nu$, were calculated from the spectral shift of the 0–0 band (see Figure 1) and are listed in Table II. The $\Delta\nu$'s calculated from the spectral shift of the phosphorescence bands are about 2.5 times larger than σ, except for the case of P(NPMA-*co*-MMA). This indicates that the triplet exciton migrates to deeper trap sites and deactivates in a photostationary condition. Therefore, the value σ represents the magnitude of interchromophore interaction in polymer matrices.

Figure 8 shows a time dependence of the excitation energy distribution calculated by Monte Carlo simulation at 135 K, where σ is taken to be 400 cm^{-1}. After 1 ms, the distribution width becomes 173 cm^{-1} and the center of distribution is located at -564 cm^{-1}. The width is narrower than half of the initial width within only 1 ms. This indicates that the triplet exciton moves quickly to a deeper trap site. Taking into account the long lifetime of the triplet state, most of the phosphorescence arises from these deeper trap sites. It should be noted that there is a discrepancy between the DOS model and the real system. As mentioned previously, the $\Delta\nu$ values are found to be around 2.5σ. Using this and the mean value of distribution

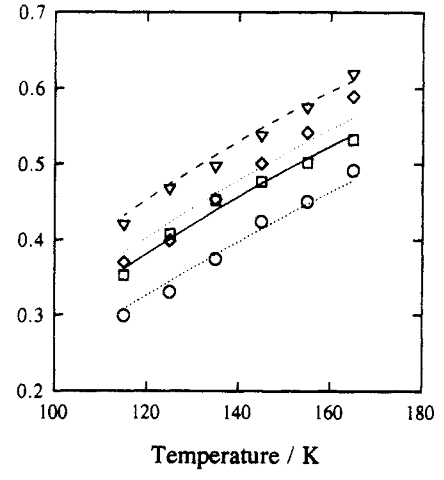

Figure 7. Plot of α vs temperature for each sample. (▽) P(NMMA-*co*-MMA), (□) P(NEMA-*co*-MMA), (◇) P(NPMA-*co*-MMA), and (○) P(PhMMA-*co*-MMA). The lines represent the result of curve fitting according to eq 7.

Table II
Width of the Gaussian Distribution, σ, and Spectral Shift of Phosphorescence, $\Delta\nu$

	σ (cm^{-1})	$\Delta\nu^a$ (cm^{-1})	$\Delta\nu/\sigma$
P(NMMA-*co*-MMA)	366	918	2.5
P(NEMA-*co*-MMA)	424	918	2.2
P(NPMA-*co*-MMA)	406	1368	3.4
P(PhMMA-*co*-MMA)	479	1221	2.5

[a] Calculated from the spectral shift of the phosphorescence 0–0 band compared with those of monomeric model compounds in MTHF at 77 K.

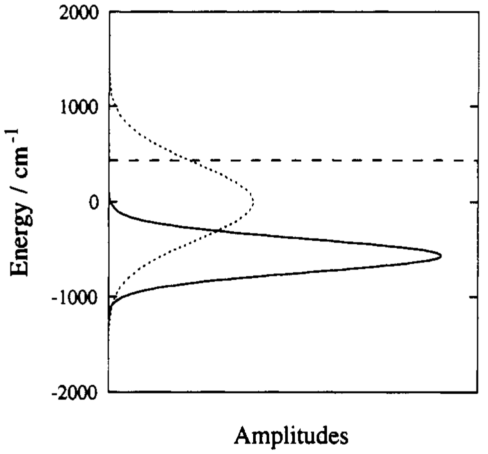

Figure 8. Change of dispersion calculated by Monte Carlo simulation. The dotted line represents an initial dispersion with a width σ = 400 cm^{-1}. The solid line represents that after 1 ms at 135 K. The width is 173 cm^{-1}, and the center is −564 cm^{-1}. The broken line indicates the expected energy level of an isolated chromophore.

after 1 ms, 560 cm^{-1}, we can estimate the position of the 0–0 band energy for the isolated triplet state, which is drawn with a broken line in Figure 8. According to the initial distribution (dotted line in Figure 8), about 15% of the trap sites must be in higher levels than the isolated chromophore. This is irrational considering the real system. However, the DOS model is still a good approximation for describing the decay kinetics and for taking a general view of the energy migration behavior.

We tried to measure the time-resolved phosphorescence spectra, but, contrary to our expectation, a gradual spectral shift with time was not detected; i.e., the energy hopping was not detected spectroscopically. The reason is probably that the rate of energy migration is too fast, as mentioned previously. The observed rise and decay curves are the response of the transport of exciton to the acceptor site; hence, the curve is a convolution of the histogram of the transport time. The result of deconvolution of DBN phosphorescence rise and decay curves indicates that the energy migration process is almost finished within several tens of microseconds. In our spectrometer, the initial 1 ms of signal after the excitation pulse is eliminated to avoid the influence of fluorescence emission. The gradual spectral shift may be detected in low-temperature measurements or by using a faster time-resolving apparatus. These experiments are being considered.

Conclusion

Triplet energy migration in polymer matrices involving triplet trap sites has been analyzed by the DOS model kinetics. The results of the kinetic analysis are in good agreement with the experimental data over the temperature range from 115 to 165 K. This indicates that energy levels of trap sites in polymer matrices disperse in a Gaussian function, and triplet excitons migrate by hopping through these trap sites. The results of the simulation deviate from the experimental data at higher temperatures than 165 K because of the back energy transfer from the acceptor molecules. In general, thermally activated processes play an important role for the photophysics of triplet states. This is also the case in the triplet energy migration observed in our polymer matrices.

References and Notes

(1) (a) Turro, N. J. *Modern Molecular Photochemistry*; Benjamin: Menlo Park, CA, 1978; p 296. (b) Birks, J. B. *Photophysics of Aromatic Molecules*; Wiley: New York, 1970; p 518. (c) Wilkinson, F. *Quart. Rev.* **1966**, *20*, 403.
(2) (a) Guillet, J. E. *Polymer Photophysics and Photochemistry*; Cambridge University Press: Cambridge, U.K., 1985. (b) Soutar, I.; Phillips, D. *Photophysical and Photochemical Tools in Polymer Science*; Winnik, M. A., Ed.; Reidel: Dordrecht, The Netherlands, 1986. (c) Fox, R. B. *Pure Appl. Chem.* **1972**, *30*, 87.
(3) Dexter, D. L. *J. Chem. Phys.* **1953**, *21*, 836.
(4) Förster, Th.; Kasper, K. *Z. Electrochem.* **1955**, *59*, 976.
(5) Vala, M. T., Jr.; Haebig, J.; Rice, S. A. *J. Phys. Chem.* **1965**, *42*, 886.
(6) (a) Hirayama, F. *J. Chem. Phys.* **1965**, *42*, 3163. (b) Zachariasse, K.; Kühnle, W. *Z. Phys. Chem.* (*Munich*) **1976**, *101*, 267.
(7) Nishijima, Y. *J. Polym. Sci. C* **1970**, *31*, 353.
(8) Ito, S.; Yamamoto, M.; Nishijima, Y. *Bull. Chem. Soc. Jpn.* **1981**, *54*, 35.
(9) Klöpffer, W.; Fischer, D. *J. Polym. Sci. C* **1973**, *40*, 43.
(10) Gijzeman, O. L. J.; Langelaar, J.; Van Voorst, J. D. W. *Chem. Phys. Lett.* **1970**, *5*, 269.
(11) Itoh, Y.; Webber, S. E. *Macromolecules* **1990**, *23*, 5065.
(12) Ito, S.; Katayama, H.; Yamamoto, M. *Macromolecules* **1988**, *21*, 2456.
(13) Katayama, H.; Ito, S.; Yamamoto, M. *J. Photopolym. Sci. Technol.* **1991**, *4*, 217.
(14) Ito, S.; Numata, N.; Katayama, H.; Yamamoto, M. *Macromolecules* **1989**, *22*, 2207.
(15) Katayama, H.; Tawa, T.; Ito, S.; Yamamoto, M. *J. Chem. Soc., Faraday Trans 2* **1992**, *88*, 2743.
(16) Bässler, H. *Phys. Status Solidi B* **1981**, *107*, 9.
(17) Kohlnaush, R. *Ann. Phys.* (*Leipzig*) **1847**, *12*, 393.
(18) El-Sayed, F. E.; MacCallum, J. R.; Pomery, P. J.; Shepherd, T. M. *J. Chem. Soc., Faraday Trans. 2* **1979**, *75*, 79.
(19) (a) Zumofen, G.; Blumen, A.; Klafter, J. *J. Chem. Phys.* **1985**, *82*, 3198. (b) Zumofen, G.; Blumen, A.; Klafter, J. *J. Chem. Phys.* **1986**, *84*, 6679.
(20) Lin, Y.; Nelson, M. C.; Hanson, D. M. *J. Chem. Phys.* **1987**, *86*, 1586.
(21) Lin, Y.; Dorfman, R. C.; Fayer, M. D. *J. Chem. Phys.* **1988**, *90*, 159.
(22) (a) Byers, J. D.; Friedrichs, M. S.; Friesner, R. A.; Webber, S. E. *Macromolecules* **1988**, *21*, 3402. (b) Byers, J. D.; Parsons, W. S.; Friesner, R. A.; Webber, S. E. *Macromolecules* **1990**, *23*, 4835.
(23) Harman, L. A.; Kopelman, R. *J. Phys. Chem.* **1990**, *94*, 3454.
(24) Li, C. S.; Kopelman, R. *Macromolecules* **1990**, *23*, 2223.
(25) (a) Yamazaki, I.; Tamai, N.; Yamazaki, T. *J. Phys. Chem.* **1990**, *94*, 516. (b) Tamai, N.; Yamazaki, T.; Yamazaki, I. *Can. J. Phys.* **1990**, *68*, 19.
(26) Janse van Rensburg, E. J.; Guillet, J. E.; Whittington, S. G. *Macromolecules* **1990**, *22*, 4212.
(27) Sienicki, K.; Durocher, G. *Macromolecules* **1991**, *24*, 1102.
(28) Kost, S. H.; Breuer, H. D. *Ber. Bunsen-Ges Phys. Chem.* **1991**, *95*, 480.
(29) (a) Richert, R.; Ries, B.; Bässler, H. *Philos. Mag. B* **1984**, *49*, 25. (b) Richert, R.; Bässler, H. *J. Chem. Phys.* **1986**, *84*, 3567.
(30) (a) Richert, R.; Elshner, A.; Bässler, H. *Z. Phys. Chem.* (*Munich*) **1986**, *149*, 63. (b) Schönherr, G.; Bässler, H.; Silver, M. *Philos. Mag. B* **1981**, *44*, 47.
(31) Inami, A.; Morimoto, K.; Murakami, Y. *Nippon Kagaku Zasshi* **1964**, *85*, 880.